Binary fluid convection as a 2×2 matrix problem

Laurette S. Tuckerman

Laboratoire d'Informatique pour la Mécanique et les Sciences de l'Ingénieur (LIMSI-CNRS)
BP 133, 91403 Orsay Cedex, France
email: laurette@limsi.fr

Introduction

Convection due to two competing or cooperating mechanisms, displays a fascinating variety of dynamical phenomena [1]. One of the physical mechanisms is usually a thermal gradient, and the other may be as diverse as a concentration, rotation, or magnetic field gradient. The transition from a conductive to a convective state is via either a steady or a Hopf bifurcation; the point separating the two was one of the first codimension-two points explored [2] The bifurcation may be super or sub-critical, and the convection amplitude may undergo a transition from weak to strong. We show [3] that all of these features can be explained as manifestations of the behavior of the eigenvalues of generic 2×2 matrix near the point where the eigenvalues intersect.

Consider a 2×2 matrix

$$\begin{pmatrix} \sigma_T & \alpha \\ \beta & \sigma_C \end{pmatrix} \tag{1}$$

whose entries depend on some control parameter r. Its eigenvalues are

$$\sigma_\pm = \frac{\sigma_T + \sigma_C}{2} \pm \sqrt{\left(\frac{\sigma_T - \sigma_C}{2}\right)^2 + \alpha\beta} \ . \tag{2}$$

The **coupling** is the product $\alpha\beta \sim S$ of the off-diagonal terms. Its sign determines the nature of the eigenvalues at $r = r_{\rm int}$, where $\sigma_T(r)$ and $\sigma_C(r)$ intersect, as shown in figure 1. If the coupling is positive, then the eigenvalues undergo avoided crossing: the eigenvalues remain real and distinct. If the coupling is negative, then the eigenvalues coalesce into a complex conjugate pair over some interval surrounding $r_{\rm int}$.

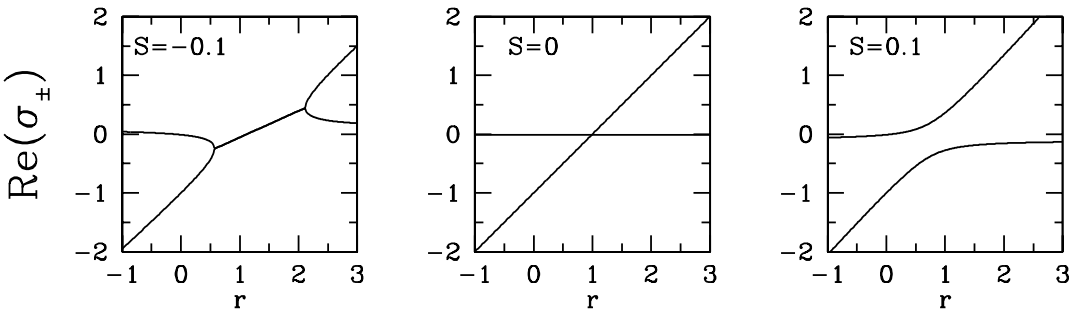

Figure 1: Real part of eigenvalues $\sigma_\pm$ of 2×2 matrix as a function of control parameter r for different signs of coupling S (product of off-diagonal terms).
$S < 0$**:** complex coalescence, i.e. formation of complex conjugate pair (real part shown).
$S = 0$**:** eigenvalues cross transversely. $S > 0$**:** avoided crossing.

Simple Model: 2D Thermosolutal Problem

We now show how the equations for binary fluid convection can be reduced to eigenvalue problems for matrices like (1), displaying the behavior shown in fig. 1. We use the simple model of two-dimensional thermosolutal convection, for which both vertical thermal and solutal gradients are imposed, with free-slip boundaries [4], as shown in figure 2. In convection in binary fluids with Soret effect, only the temperature gradient is imposed, but cross diffusion induces a concentration gradient with similar properties [5]. The fluid is Boussinesq, with density

$$\rho(T,C) = \rho_0 + \rho_T(T - T_0) + \rho_C(C - C_0). \tag{3}$$

The temperature and concentration are set to T_0, C_0 at $z = 0$ and to $T_0 - \Delta T, C_0 - \Delta C$ at $z = h$.

The three diffusivities – the thermal diffusivity κ_T, the solute diffusivity κ_C, and the kinematic viscosity ν – are described by two nondimensional ratios, the Prandtl number $P = \nu/\kappa_T$ and the Lewis number $L = \kappa_C/\kappa_T$. We take as the two remaining nondimensional parameters the Rayleigh number R and the separation ratio S defined by

$$R \equiv \frac{g\rho_T \Delta T h^3}{\nu \kappa_T} \qquad S \equiv \frac{\rho_C \Delta C}{\rho_T \Delta T} \tag{4}$$

We fix $L \ll 1$ and $P \gg 1$ and vary R and S.

The velocity is represented by a streamfunction $\mathbf{U} = \nabla \times \phi(x,z)\mathbf{e}_y$, obeying periodic boundary conditions $\phi(0,z) = \phi(\lambda,z)$ in x and free-slip boundary conditions $\phi = \partial_{zz}\phi = 0$ at $z = 0,\ h$. There exists a motionless conductive solution $T = T_0 - z\Delta T$, $C = C_0 - z\Delta C$, $\mathbf{U} = \nabla \times \phi \mathbf{e}_y = 0$.

We subtract the conductive solution and nondimensionalize. The governing equations are then

$$\partial_t \hat{T} = \partial_x \hat{\phi} + \mathbf{e_y} \cdot (\nabla\hat{\phi} \times \nabla\hat{T}) + \nabla^2 \hat{T} \tag{5a}$$

$$\partial_t \hat{C} = \partial_x \hat{\phi} + \mathbf{e_y} \cdot (\nabla\hat{\phi} \times \nabla\hat{C}) + L\nabla^2 \hat{C} \tag{5b}$$

$$\partial_t \nabla^2 \hat{\phi} = PR\partial_x(\hat{T} + S\hat{C}) + \mathbf{e_y} \cdot (\nabla\hat{\phi} \times \nabla\nabla^2\hat{\phi}) + P\nabla^4\hat{\phi}. \tag{5c}$$

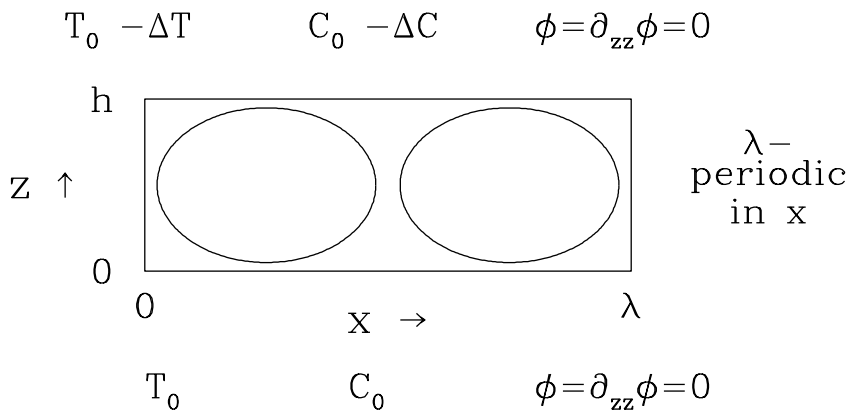

Figure 2: 2D thermsolutal problem with periodic BCs in x and free-slip BCs in z.

Linear Analysis:

We begin by carrying out a linear stability analysis of (5). The simplicity of the free-slip problem leads to linear eigenmodes of the form

$$\left\{ \begin{array}{c} \hat{T} \\ \hat{C} \\ \hat{\phi} \end{array} \right\}(x,z,t) = \left\{ \begin{array}{c} T\cos(kx) \\ C\cos(kx) \\ \phi\sin(kx) \end{array} \right\} \sin(\pi z)\exp((k^2+\pi^2)\sigma t) \tag{6}$$

We fix k at the critical wavenumber $k \equiv \pi/\sqrt{2}$ and define $\gamma^2 \equiv k^2+\pi^2$ and $r \equiv Rk^2/\gamma^6$. If $P=\infty$ then (5c) becomes the algebraic equation $\phi = -r(T+SC)\gamma^2/k$, permitting the elimination of ϕ.

By substituting (6) into (5), we obtain the following 2×2 system for the amplitudes (T,C):

$$\sigma \left(\begin{array}{c} T \\ C \end{array} \right) = \left(\begin{array}{cc} r-1 & rS \\ r & rS-L \end{array} \right) \left(\begin{array}{c} T \\ C \end{array} \right). \tag{7}$$

The situation is like that of 1 and fig. 1. We can identify the first diagonal element as a "thermal" eigenvalue $\sigma_T = r-1$ with threshold $r_T = 1$ and the second diagonal element as a "solutal" eigenvalue $\sigma_C = rS-L$ with threshold $r_C = L/S$. The "thermal" and "solutal" eigenvalues are coupled by Sr^2. They cross transversely at their intersection point $r_{\rm int} = (1-S)/(1-L)$ if $S=0$, undergo avoided crossing if $S>0$ and complex coalescence if $S<0$.

The eigenvalues of (7) are

$$\begin{aligned} \sigma_\pm = \frac{(r-1)+(rS-L)}{2} &\pm \sqrt{\left(\frac{(r-1)-(rS-L)}{2}\right)^2 + Sr^2} \\ &\equiv f_L \pm \sqrt{g_L} \end{aligned} \tag{8}$$

We rederive the classic results by inverting (8):

$$r = \frac{\sigma_\pm^2 + \sigma_\pm(1+L)+L}{\sigma_\pm(1+S)+(S+L)}. \tag{9}$$

Each value of σ corresponds to a unique value of r. In particular, unless $S=-L$, there is exactly one pitchfork bifurcation $\sigma=0$ at

$$r = r_{PF} = \frac{L}{S+L}. \tag{10}$$

If $S<0$, eigenvalues are complex over the range where $g_L<0$:

$$\frac{1-L}{(1+\sqrt{-S})^2} \equiv r_{c-} < r < r_{c+} \equiv \frac{1-L}{(1-\sqrt{-S})^2} \tag{11}$$

There is a Hopf bifurcation if $f_L=0$ in this range, i.e. if $-1<S<-L^2$:

$$r_{\rm H} = \frac{1+L}{1+S} \qquad w_{\rm H}^2 = -\frac{S+L^2}{1+S} \tag{12}$$

At $S=-1$, $r_{\rm H}\to\infty$. At

$$S_* \equiv -L^2 \qquad r_* \equiv \frac{1}{1-L} \tag{13}$$

the Hopf frequency $\omega_{\rm H}$ goes to zero. That is, $r_{\rm H}$ disappears at the well-known Takens-Bogdanov codimension-two point [2] by coalescing with the pitchfork bifurcation when $f_L = g_L = 0$; see figure 3.

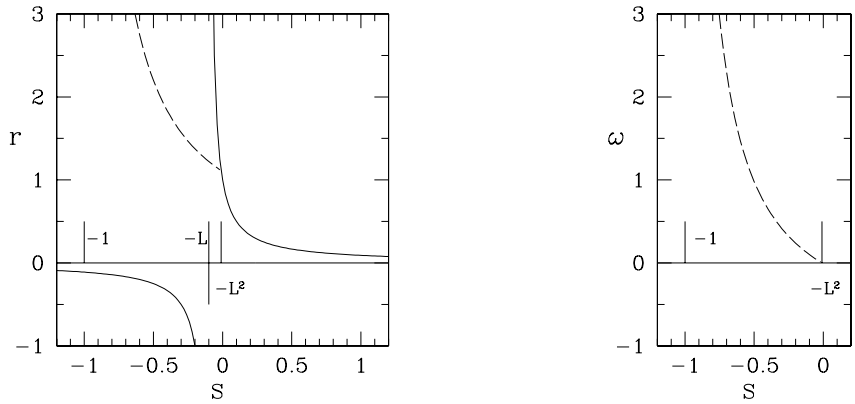

Figure 3: Left: Thresholds for pitchfork ($r_{\rm PF}$, solid curves) and Hopf bifurcations ($r_{\rm H}$, dashed curve) as a function of S. Short lines segments indicate limits $S = -L$ for $r_{\rm PF}$ and $S = -1$, $S = -L^2$ for $r_{\rm H}$. Right: Frequency ω for Hopf bifurcation.

Nonlinear analysis:

When (6) is substituted into the full thermosolutal equations (5), the nonlinear interactions generate terms of the form

$$\left\{ \begin{array}{c} T_2 \\ C_2 \end{array} \right\} \sin(2\pi z). \tag{14}$$

We add terms of the form (14) to (6), substitute into (5), and neglect higher-order trigonometric terms. This procedure, analogous to the derivation of the classic Lorenz model [6] for pure thermal convection, yields the five-variable Veronis model [4]:

$$\partial_t \left(\begin{array}{c} T \\ C \\ \phi \\ T_2 \\ C_2 \end{array} \right) = \left(\begin{array}{ccccc} -\gamma^2 & 0 & -k & 0 & 0 \\ 0 & -L\gamma^2 & -k & 0 & 0 \\ -P\gamma^4 r/k & -PS\gamma^4 r/k & -P\gamma^2 & 0 & 0 \\ 0 & 0 & 0 & -4\pi^2 & 0 \\ 0 & 0 & 0 & 0 & -L4\pi^2 \end{array} \right) \left(\begin{array}{c} T \\ C \\ \phi \\ T_2 \\ C_2 \end{array} \right) + \left(\begin{array}{c} -\pi k \phi T_2 \\ -\pi k \phi C_2 \\ 0 \\ \frac{\pi k}{2} \phi T \\ \frac{\pi k}{2} \phi C \end{array} \right) \tag{15}$$

We seek steady states of the Veronis model (15). T_2, C_2, and ϕ can be eliminated to yield

$$\left(\begin{array}{cc} r-1 & rS \\ Lr & L(rS-L) \end{array} \right) \left(\begin{array}{c} T \\ C \end{array} \right) = \frac{1}{2} \left(\frac{r\gamma}{2} \right)^2 (T + SC)^2 \left(\begin{array}{c} T \\ C \end{array} \right) \tag{16}$$

The reduction of (15) to (16) does not require P to be small. The notable feature of (16) is that it too has the form of an eigenvalue problem, with the square amplitude or energy

$$E \equiv A^2 \equiv \frac{1}{2} \left(\frac{r\gamma}{2} \right)^2 (T + SC)^2 \tag{17}$$

playing the role of an eigenvalue. Thus, the nonlinear problem (16) can be solved by diagonalizing the matrix on the left-hand-side. The eigenvalues give the values of A^2, and the corresponding eigenvectors can be used to express one of T, C as a function of the other.

A related version of this reduction has been shown [7, 8] to be valid for the full PDEs governing binary fluid convection with Soret effect with realistic boundary conditions. These authors demonstrate that the velocity field can be well approximated by a single spatial mode and can be adiabatically eliminated, yielding a linear system for the temperature and concentration amplitudes.

The energy problem (16) is very similar to the growth-rate problem (7). Solutions to (16) are

$$A^2 = \frac{(r-1)+L(rS-L)}{2} \pm \sqrt{\left(\frac{(r-1)-L(rS-L)}{2}\right)^2 + SLr^2}$$
$$\equiv f_{NL}(r) \pm \sqrt{g_{NL}(r)}. \tag{18}$$

In fact, comparison of (16) and (7) shows a quantitative correspondence between the growth rate and energy problems. Results concerning the growth rate can be translated to energy simply via

$$\sigma \to A^2, \qquad L \to L^2, \qquad S \to LS. \tag{19}$$

There is a "thermal" steady state characterized by $A_T^2 = (r-1)$ and a "solutal" steady state $A_C^2 = L(rS-L)$, with a coupling strength of SLr^2. These states undergo avoided crossing or complex conjugation according to the sign of S, as shown in figure 4. However, the interpretation differs.

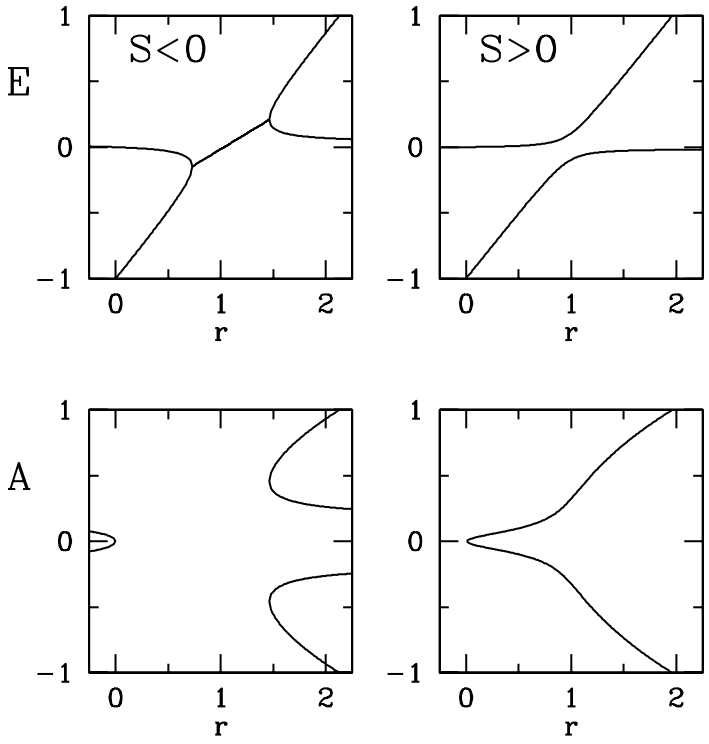

Figure 4: Re(A^2) and A as a function of r for different signs of coupling.
Complex coalescence $S < 0$**:** Transition from complex to positive real A^2 corresponds to creation of two pairs of real solutions A, i.e. a pair of saddle-node bifurcations.
Avoided crossing $S > 0$**:** Change in slope of A^2 corresponds to change of curvature in A between weak solutal and strong thermal convective regimes.

For $S < 0$, there is a range over which A^2 is complex. Whereas complex or negative values for the growth rate σ indicate oscillating or decaying transients, only real and positive values of A^2 are meaningful. The transition from complex to positive real A^2 corresponds to the creation of two pairs of real solutions A, i.e. a pair of saddle-node bifurcations as shown on

the left of fig. 4. The substitution (19) applied to (11) and the requirement of positive real A^2 show that a saddle-node bifurcation occurs at

$$r_{\rm SN} = \frac{1-L^2}{(1-\sqrt{-LS})^2} \quad \text{if} \quad -\frac{1}{L} < S < -L^3. \tag{20}$$

There is a codimension-two point for A^2 at which the saddle-node and pitchfork bifurcations coincide, i.e. $f_{\rm NL} = g_{\rm NL} = 0$. At this point, the pitchfork bifurcation is degenerate, neither supercritical nor subcritical. This codimension-two point corresponds to that obtained for the growth rate σ at which the Hopf and pitchfork bifurcations coincide. The substitution (19) applied to (13) yields

$$\tilde{S}_* = -L^3 \quad \tilde{r}_* \equiv \frac{1}{1-L^2}. \tag{21}$$

For $S > 0$, avoided crossing corresponds to a fairly abrupt transition between a low-amplitude solutal regime and a high-amplitude thermal regime, as seen in on the right of fig. 4. This transition was derived for the five-variable model [9] and was observed experimentally [10, 11]; the two regimes were termed the Soret and Rayleigh regimes, respectively. The transition may be gradual or may occur for a negative value of A^2; we find that the Soret-to-Rayleigh transition is observable over the range $L \lesssim S \lesssim 1$.

Lorenz-like Hybrid Model

Finally, we can combine (7) and (16) into a single two-dimensional dynamical system:

$$\frac{1}{\gamma^2}\frac{d}{dt}\begin{pmatrix} T \\ C \end{pmatrix} = \begin{pmatrix} r-1 & rS \\ r & rS-L \end{pmatrix}\begin{pmatrix} T \\ C \end{pmatrix} - \frac{1}{2}\left(\frac{r\gamma}{2}\right)^2 (T+SC)^2 \begin{pmatrix} 1 & 0 \\ 0 & 1/L \end{pmatrix}\begin{pmatrix} T \\ C \end{pmatrix}. \tag{22}$$

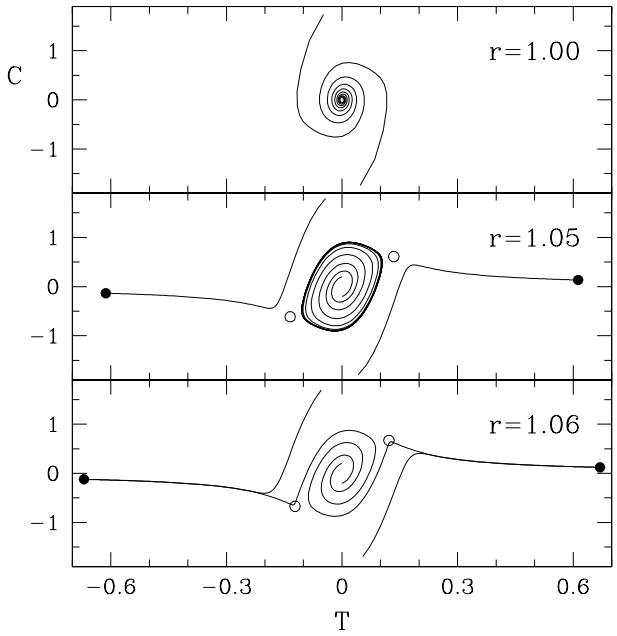

Figure 5: Phase portraits illustrating heteroclinic bifurcation for $S = -L = -0.01$. For $r = 1.00$, all trajectories spiral into $(T, C) = (0, 0)$. For $r = 1.05$, trajectories either spiral out to a limit cycle or terminate on one of the stable steady states (solid dots) after being deflected by one of the saddle points (hollow dots). For $r = 1.06$, the limit cycle has been destroyed by colliding with the saddle points in a heteroclinic bifurcation.

$S = 0$ is an *organizing center* for (22). By construction, (22) reproduces the linear stability diagram and the nonlinear steady states. It also describes the limit cycle created by the Hopf bifurcation, which is annihilated by colliding with the unsteady states emanating from the saddle-node bifurcation at $r_{\rm SN}$ in a global heteroclinic bifurcation [12] as illustrated in figure 5. Referring to (6), the limit cycle of fig. 5 is a standing wave solution of the partial differential equations (5). In treatments of binary fluid convection adapted to large or infinite horizontal domains, in which the phases of the various components are allowed to vary, then the Hopf bifurcation gives rise to a branch of stable traveling waves which disappears via a drift bifurcation by meeting the branch of stable steady states; the standing waves described above continue to exist but are unstable [13, 14]. These traveling waves are inaccessible to our simplified model, as are other spatial patterns found in binary fluid convection such as pulses [15], square patterns [10, 11], and modulated traveling waves [14]; and temporal dynamics found in reduced models, such as period-doubling and chaos [12].

References

[1] W. Barten, M. Lücke, M. Kamps & R. Schmitz 1995, *Convection in binary fluid mixtures. I. Extended traveling-wave and stationary states*, Phys. Rev. E **51**, 5636;
II. Localized traveling waves, Phys. Rev. E 51, 5662.

[2] E. Knobloch & M.R.E. Proctor 1981, *Nonlinear periodic convection in double-diffusive systems*, J. Fluid Mech. **108**, 291.

[3] L.S. Tuckerman 2001, *Thermosolutal and binary fluid convection as a 2×2 matrix problem*, Physica D **156**, 325.

[4] G. Veronis 1965, *On finite amplitude instability in thermohaline convection*, J. Mar. Res. **23**, 1.

[5] E. Knobloch 1980, *Convection in binary fluids*, Phys. Fluids **23**, 1918.

[6] E.N. Lorenz 1963, *Deterministic non-periodic flows*, J. Atmos. Sci. **20**, 130.

[7] St. Hollinger & M. Lücke 1998, *Influence of the Soret effect on convection of binary fluids*, Phys. Rev. E **57**, 4238.

[8] St. Hollinger, M. Lücke & H.W. Müller 1998, *Model for convection in binary liquids*, Phys. Rev. E **57**, 4250.

[9] J.K. Platten & G. Chavepeyer 1976, *Instabilité et flux de chaleur dans le problème de Bénard à deux constituants aux coefficients de Soret positifs*, Int. J. Heat Mass Transfer **19**, 27.

[10] P. Le Gal, A. Pocheau & V. Croquette 1985, *Square versus roll patern at convective threshold*, Phys. Rev. Lett. **54**, 2501.

[11] E. Moses & V. Steinberg 1986, *Competing patterns in a convective binary mixture*, Phys. Rev. Lett. **57**, 2018.

[12] L.N. Da Costa, E. Knobloch & N.O. Weiss 1981, *Oscillations in double-diffusive convection*, J. Fluid Mech. **109**, 25.

[13] P. Coullet, S. Fauve & E. Tirapegui 1985, *Large scale instability of nonlinear standing waves*, J. Phys. (Paris) Lett. **46**, L787.

[14] E. Knobloch 1986, *Oscillatory convection in binary mixtures*, Phys. Rev. A **34**, 1538.

[15] W. Barten, M. Lücke, M. Kamps & R. Schmitz 1995, *Convection in binary fluid mixtures. II. Localized traveling waves*, Phys. Rev. E 51, 5662.